Measuring Glide-Reflection Symmetry in Human Movements Using Elastic Shape Analysis

Qiao Wang[1,2]   Chaitanya Potaraju[1]   Pavan Turaga[2,1]

[1] School of Electrical, Computer and Energy Engineering
[2] School of Arts, Media and Engineering
Arizona State University, Tempe, Arizona, USA

{qiao.wang, cpotaraj, pturaga}@asu.edu

Abstract

Human bodies and movements exhibit inherent symmetry. However, an important class of everyday movements, such as walking, does not maintain symmetry at every time instance. The symmetry in these movements is a spatio-temporal glide-reflection symmetry. The ability to measure this type of symmetry will provide us opportunities for various computer-aided applications including health monitoring, rehabilitation, and athletic training. In this paper we propose a method that uses the tools from elastic shape analysis to provide continuous symmetry scores which measure the degree of glide-reflection symmetry in movements. These scores can be updated online after each frame, and easily combined to drive comprehensible feedback. Our preliminary experiment demonstrates that our symmetry scores can well distinguish between a normal gait and simulated stroke and Parkinsonian gaits. Our results also suggest that using the Riemannian elastic metric provides better scores than Euclidean approaches.

1. Introduction

Human bodies are bilaterally symmetric, and this spatial symmetry is preserved in many everyday postures and actions. However, there is an important class of movements in which this spatial symmetry is not maintained throughout the duration of the whole movement but still commonly considered as symmetric. Walking, running, crawling, and certain styles of swimming (front crawl, backstroke) are all examples of this type. The perceived symmetry in these movements is not purely spatial but spatio-temporal, and can also be described as a glide-reflection symmetry, in which an invariance or approximate invariance exists with
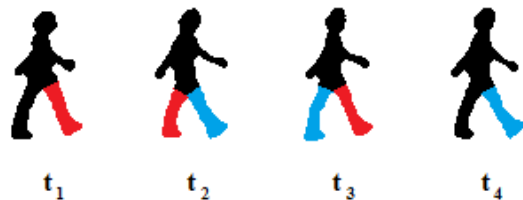
Figure 1: An example of spatio-temporal glide-reflection symmetry in walking between the right leg (red) and the left leg (blue).

regard to the combination of a temporal glide and a spatial reflection.

Figure 1 illustrates an example of this spatio-temporal glide-reflection symmetry (using silhouettes from the Weizmann dataset [4]). The trajectory of the right leg (colored in red) is spatially symmetric with the left leg (colored in blue), but only after a temporal glide. The left and right legs are not in spatially symmetric positions except at certain time instances, nor are their trajectories reflections of each other in the same time period (*e.g.* from t_1 to t_3). However, the trajectory of the right leg is approximately the spatial reflection of that of the left leg in a different time period. In the example given in Figure 1, the trajectory of the right leg from t_1 to t_3 and that of the left leg from t_2 to t_4 are symmetric across the median plane. Similar symmetry exists in the arm movements. This type of symmetry cannot be found by only looking at spatial or temporal relationships between different body parts, but has to be considered using the combination of both.

While a normal, healthy person's walking usually exhibits a high degree of glide-reflection symmetry, it may not always be the case when the person's motor function

deteriorates. There also exist movements which may be learned in adulthood and can exhibit varying degrees of glide-reflection symmetry (*e.g.* swimming). Therefore, it is useful to quantify how much such a movement deviates from perfect glide-reflection symmetry. In this paper, we propose a method for this purpose, with an aim for obtaining continuous, online, and potentially real-time, symmetry scores. These scores can then be used in computer systems for various applications, such as health monitoring, multimedia rehabilitation, and computer-aided athletic training.

An example of such a feedback system for spatial reflection symmetry was previously developed [16], inspired by a rehabilitation program for stroke patients [1]. When using this feedback system, a spatial symmetry score is computed based on the locations of selected body joints in each frame, obtained from a Microsoft Kinect sensor. A continuous auditory feedback is then generated from this symmetry score. In this particular design, higher symmetry scores generate more prominent musical feedback, while lower scores do the opposite. Therefore the user can adjust their posture or movement (*e.g.* sit-to-stand) to be more symmetric, based on the continuous, real-time feedback they receive. This system however is not useful for movements with glide-reflection symmetry such as walking, because even with highly symmetric walking, high spatial symmetry is only achieved at certain time instances, but not during the whole movement. The spatial symmetry score will fluctuate cyclically in a wide range, making the resulting fast changing feedback too difficult for a human user to mentally process (an example is given in Figure 2). Therefore, it is useful
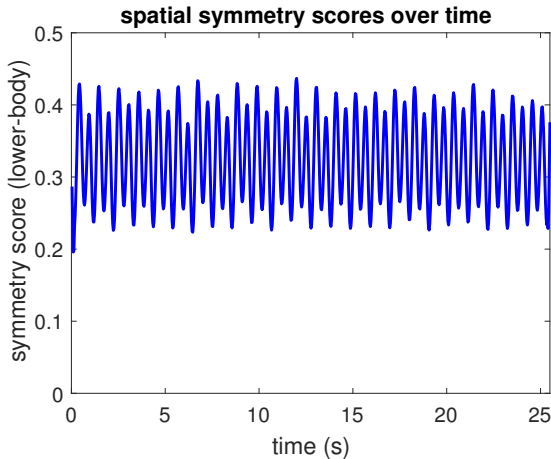

Figure 2: Spatial symmetry scores computed from a normal walking sequence, using Euclidean distances in each frame, between the locations of the left knee and foot and those of the right knee and foot after a reflection through the median plane.

to have a method that obtains stable symmetry scores for movements with glide-reflection symmetry, such that the score itself, not its changing pattern, reflects how symmetric a movement is. In this paper, we compute these symmetry scores using the tools from elastic shape analysis [12], and our preliminary experiment suggests that our method may provide better symmetry scores than similar approaches using Euclidean distances.

2. Related work

The concept of glide-reflection symmetry is not new [3, 11]. However, though frequently studied by mathematicians and physicists, analyzing glide-reflection symmetry in computer vision is not common. An early successful effort was made by Y. Liu *et al.* [9], which used frieze patterns to analyze parameters from gait sequences. A more recent study [8] expanded the concept into curved glide-reflection symmetry and proposed a method to detect the existence of such symmetry in 2D and 3D images. Most of the related existing work focused on detecting such symmetry and locating the symmetry axis/plane, and as far as we know, the problem of quantifying glide-reflection symmetry, especially with regard to human movements, has rarely been investigated.

There was prior work in quantifying spatial symmetry [10, 15] or temporal symmetry [14] from the entirety of an object or movement. Elastic shape analysis has also been used to generate spatially symmetric shapes [10] or temporally symmetric animations [2]. However, as discussed above, the spatio-temporal glide-reflection symmetry can only be analyzed when combining the spatial and temporal domains together.

The movements of walking and running have been extensively studied by biomedical researchers, and the field is known as gait analysis. Gait analysis can be qualitatively done by visual inspection from clinicians. Quantitatively, gait analysis analyzes the spatio-temporal relationships in gait by measuring parameters from repeated gait cycles (*e.g.* [17]). However, these parameters usually only consider discrete cyclic events (*e.g.* foot leaving the ground) and ignore the whole movements between them. The measures are usually only updated after each gait cycle, and therefore have significant limitation for the applications we aspire to develop.

3. Mathematical framework

A human movement can be described by the trajectories of various body parts. Each trajectory exists in the same 3-dimensional Euclidean space, and is denoted by $p_* : [T_1, T_2] \rightarrow \mathbb{R}^3$, where "*" corresponds to a specific body part (*e.g.* "right hand"). These trajectories can be obtained from various sources, such as

motion capture systems, depth sensors, or pose estimation from single or multiple RGB cameras. The movement of the whole body is then described by the set of all relevant trajectories $\{(p_a(t)), (p_b(t)), \dots\}$. To measure glide-reflection symmetry, we need to have trajectories of corresponding body parts on both sides of the body (*e.g.* left hand and right hand) in the form of $\{(p_{l\_a}(t)), (p_{r\_a}(t)), (p_{l\_b}(t)), (p_{r\_b}(t)), \dots\}$.

As discussed in the Introduction section, a symmetry score for glide-reflection symmetry should compare a segment of trajectory on one side with the spatially reflected version of a temporally glided segment on the other side. Since we want to obtain online and potentially real-time symmetry scores, at time $t \in [T_1, T_2]$, we will have access to current and history data $[T_1, t]$, but not future data $(t, T_2]$. For the current symmetry score A at time t, the segment of trajectory on that "one side" should be the most current version (*i.e.* from $[t-T, t]$). Since we can choose both left and right side as the "one side", there are two symmetry scores here, one comparing the latest segment from the left side with a past segment from the right side, and the other vice versa. We denote these two scores $A_{(l)}$ and $A_{(r)}$ respectively, and intuitively these two scores should be close to each other over the course of the whole movement.

For the simplicity of expression, we first pick just one pair of body parts, whose trajectories are $p_l(t)$ and $p_r(t)$, and their symmetry scores are:

$$A_{(l)}(t) = d\left(\left(p_l(\tau) \right)_{\tau=t-T}^{t}, \left(R_{(l)}^* \circ G_{(l)}^* \left(p_r(\tau) \right) \right)_{\tau=t-T}^{t} \right) \tag{1}$$

$$A_{(r)}(t) = d\left(\left(p_r(\tau) \right)_{\tau=t-T}^{t}, \left(R_{(r)}^* \circ G_{(r)}^* \left(p_l(\tau) \right) \right)_{\tau=t-T}^{t} \right) \tag{2}$$

where R^* is the optimal spatial reflection, and G^* is the optimal temporal glide (given the parameters t, T, *etc.*), both of which will be discussed later in this section, and d is a distance function between two segments of trajectories. For the purpose of being concise, below we only discuss further about $A_{(l)}(t)$, and the reader can easily apply the equations similarly to $A_{(r)}(t)$.

The choice for proper values of T needs to be considered. In theory the entirety of history data from T_1 to t are available for use. However, using too much of them may not be optimal, because it can be both computationally costly and also undesirable in the context of real-time applications to have scores influenced by signals from the remote past. Conversely, T values that are too small may yield noisy scores. Since movements with glide-reflection symmetry are often also periodic, a natural choice is to use the fundamental period as T. This value may change over the course of a movement (*e.g.* a person can adjust the speed of their walking), in which case T can be treated as a function of t and updated frequently. Alternatively, using a fixed

T value, especially in the absence of periodicity, is also a viable option.

There are also various choices for the distance function d. In our framework, we consider the trajectories ($p_l(t)$ and $p_r(t)$) as open curves on Kendall's shape manifold [7], *i.e.* trajectories form equivalent classes after removing translation, rotation, and scaling. Following Kendall's approach, the geodesic distance on this manifold between the equivalent classes of two normalized and registered trajectories $p_1(t)$ and $p_2(t)$, $t \in [t_1, t_2]$ is:

$$d_s([p_1], [p_2]) = \inf_{O \in SO(3)} d_c(p_1, Op_2) \tag{3}$$

where d_c is a distance function on the sphere in $\mathbb{L}^2([t_1, t_2], \mathbb{R}^3)$.

$$d_c(p_1, p_2) = \sqrt{\int_{t_1}^{t_2} \|p_1(t) - p_2(t)\|^2 \mathrm{d}t} \tag{4}$$

We further apply the square-root velocity (SRV) representation [12] to allow additional invariance to reparameterization. The SRV function is defined as $q : [t_1, t_2] \to \mathbb{R}^3$ [12]:

$$q(t) = \dot{p}(t) / \sqrt{\|\dot{p}(t)\|} \tag{5}$$

The scores in Eqs. (1) and (2) are then calculated with q functions instead, with the following distance function:

$$d_s([q_1], [q_2]) = \inf_{(\gamma, O) \in \Gamma \times SO(3)} d_c\left(q_1, O(q_2 \circ \gamma) \sqrt{\dot{\gamma}}\right) \tag{6}$$

where $\Gamma = \{\gamma : [t_1, t_2] \to [t_1, t_2] | \gamma(t_1) = t_1, \gamma(t_2) = t_2, \gamma$ is a diffeomorphism$\}$, and similar to Eq. (4),

$$d_c(q_1, q_2) = \sqrt{\int_{t_1}^{t_2} \|q_1(t) - q_2(t)\|^2 \mathrm{d}t} \tag{7}$$

Using SRV functions, we rewrite Eq. (1) at time t as:

$$A_{(l)} = \inf_{(\gamma, O) \in \Gamma \times SO(3)} d_c\left(q_l(\tau), O(q_r^* \circ \gamma(\tau)) \sqrt{\dot{\gamma}}\right) \tag{8}$$

where $q_r^*(\tau)$ is the q function of $R^* \circ G^*\left(p_r(\tau)\right)$.

A spatial reflection R can be described with a Householder transformation [5]: $H(u) = I - 2uu^T$, where u is a unit vector in $\mathbb{R}^3$. A temporal glide G with parameter Δ changes $p(\tau)$ to $p(\tau - \Delta)$. It should be noted that Δ is a function of t, but not a function of τ, *i.e.* the optimal $\Delta^*(t')$ for symmetry score $A(t')$ can be different from the optimal $\Delta^*(t)$ for $A(t)$, but with a given t, the Δ in the following equations is to be considered a constant with regard to τ. In other words, Δ only represents the overall temporal glide between two segments — $[t-T, t]$ on one side, and $[t-\Delta-T, t-\Delta]$ on the other side. The varying temporal

glide within the segments is covered by the reparameterization function γ. Therefore using a constant Δ (with regard to τ) does not imply a constant temporal glide, but simplifies the optimization problem.

It is easy to verify that the action of any H matrix commutes with actions of Γ and those of $SO(3)$. Therefore Eq. (8) is equivalent to

$$A_{(l)} = \inf_{\Delta \in D} \inf_{(u,\gamma,O) \in \mathbf{S}^2 \times \Gamma \times SO(3)} a_{(l)(\Delta,u,\gamma,O)} \quad (9)$$

$$a_{(l)(\Delta,u,\gamma,O)} = d_c\Big(q_l(\tau), OH(u)q_r\big(\gamma(\tau)-\Delta\big)\sqrt{\dot\gamma}\Big) \quad (10)$$

where $D = [\Delta_{min}, \Delta_{max}]$ is the search range for optimal Δ.

Since $H(u)$ is orthogonal and $\det H(u) = -1$ [5], $H(u)$ can be decomposed into an arbitrary reflection, *e.g.* $R_x = \begin{bmatrix} -1 & 0 & 0 \\ 0 & 1 & 0 \\ 0 & 0 & 1 \end{bmatrix}$, and a rotation $O' \in SO(3)$ such that $H(u) = O'R_x$. O' can then be combined with O to simplify Eqs. (9) and (10) to

$$A_{(l)} = \inf_{\Delta \in D} a_{(l)(\Delta)} \quad (11)$$

$$a_{(l)(\Delta)} = \inf_{(\gamma,O) \in \Gamma \times SO(3)} a_{(l)(\Delta,\gamma,O)} \quad (12)$$

$$a_{(l)(\Delta,\gamma,O)} = d_c\Big(q_l(\tau), OR_xq_r\big(\gamma(\tau)-\Delta\big)\sqrt{\dot\gamma}\Big) \quad (13)$$

To find the optimal $A_{(l)}$, we use an approach similar to [6], in which O is calculated from SVD, and γ is computed using a dynamic programming (DP) algorithm. The difference is that here we have an additional parameter Δ. To find the optimal Δ, a gradient descent approach is used. We start from $\Delta_0 = T/2$, and $\Delta_1 > \Delta_0$. The score $a_{(l)(\Delta)}$ is updated using Eqs. (12) and (13) in each iteration, and the gradient is calculated as

$$\dot a_{(l)(\Delta)} = \frac{a_{(l)(\Delta_i)} - a_{(l)(\Delta_{i-1})}}{\Delta_i - \Delta_{i-1}} \quad (14)$$

In practice, this search usually converges within a few iterations, and gives us an optimal Δ^* and the symmetry score $A_{(l)}$ as desired.

4. Experimental results

To evaluate our proposed method, we collected walking data from a motion capture system. The actor walked on a treadmill, with 12 sets of markers on his shoulders, elbows, hands, hips, knees, and feet. The actor followed instructions on gait abnormalities from Stanford Medicine's website [13] to simulate hemiplegic (stroke) and Parkinsonian gaits. The detailed descriptions and demonstrations of these pathological gaits can be seen at [13], and Figure 3 provides simplified illustrations on the foot movements of normal and pathological gaits. For each gait type, 3 sessions
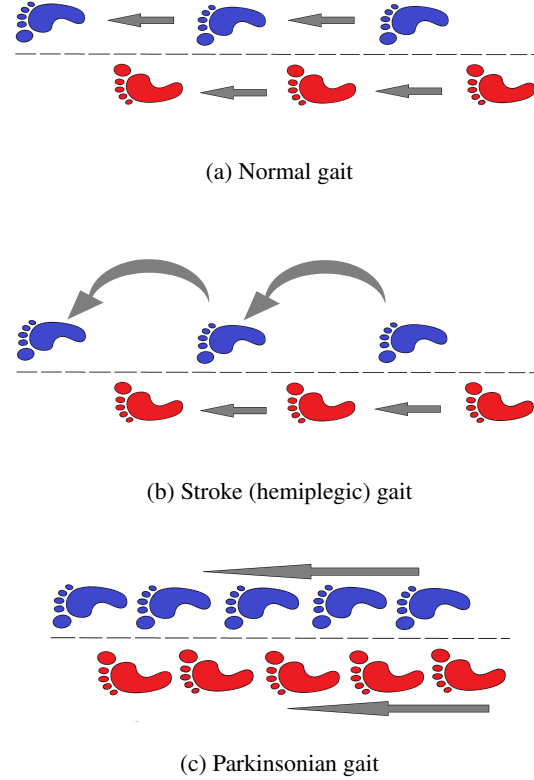

(a) Normal gait

(b) Stroke (hemiplegic) gait

(c) Parkinsonian gait

Figure 3: Illustrations of normal and pathological gaits

of data were collected, with each session $15-30$ seconds of duration, and symmetry scores calculated after the 4th second in each session. The data were capture at 120 FPS, and downsampled to 30 FPS for computation.

First, we examined the usefulness of including temporal glide in our method. As shown in Figure 2, a major problem with using only spatial reflection symmetry is that the scores fluctuate too much so that the generated feedback is difficult to comprehend. Without introducing temporal glide, this can however be mitigated by calculating spatial symmetry with consideration of temporal history — instead of using only locations in the latest frame, symmetry scores can be calculated by comparing the left and right trajectories over a period of time. Nonuniform temporal alignment between the two trajectories can also be applied (*e.g.* by using the SRV functions). Here we call this type of scores *symmetry scores without glide* $A0$, and they were calculated by similarly using Eqs. (12) and (13) but with $\Delta = 0$. By comparison, with our method, we searched for an optimal temporal glide Δ in the range of $[0, T]$.

Second, we compared the results of our method with those using Euclidean metrics. To account for speed varia-

tion, the trajectory on either side was first resampled such that the distances between adjacent sampling points were the same. The first comparing symmetry scores were calculated as:

$$A_{(l)} = \inf_{\Delta \in D} \inf_{O \in SO(3)} d_c\big(\tilde{p}_l(\tau), OR_x\tilde{p}_r(\tau - \Delta)\big) \quad (15)$$

where $\tilde{p}_l$, $\tilde{p}_r$ are the trajectories after equidistant resampling, and d_c is defined as in Eq. (4). The second comparing scores were calculated similarly but the distances were computed after dynamic time warping (DTW). $A0$ scores were also calculated using Eq. (15) but with $\Delta = 0$.

For all scores, the skeleton formed by the 12 sets of markers was first normalized and registered such that the centroid was always at the origin and the average arm length plus leg length was equal to 1. To facilitate comprehensible feedback, the scores from multiple body parts were combined into two composite symmetry scores, upper-body score A_{ub} and lower-body score A_{lb}. With our proposed method,

$$A_{ub} = \frac{L_{ua}}{2L_{ua} + L_{la}} A_{elbow} + \frac{L_{ua} + L_{la}}{2L_{ua} + L_{la}} A_{hand} \quad (16)$$

$$A_{lb} = \frac{L_{ul}}{2L_{ul} + L_{ll}} A_{knee} + \frac{L_{ul} + L_{ll}}{2L_{ul} + L_{ll}} A_{foot} \quad (17)$$

where L_{ua}, L_{la}, L_{ul}, L_{ll} were the average lengths of upper arm, lower arm, upper leg, lower leg, respectively, measured from motion capture data. Because q functions were normalized before distances were calculated, adding these coefficients in Eqs. (16) and (17) gave hands and feet more weight proportional to their ranges of motion. With Euclidean approaches, because the hands and feet already had larger ranges of motion in p_l and p_r than the elbows
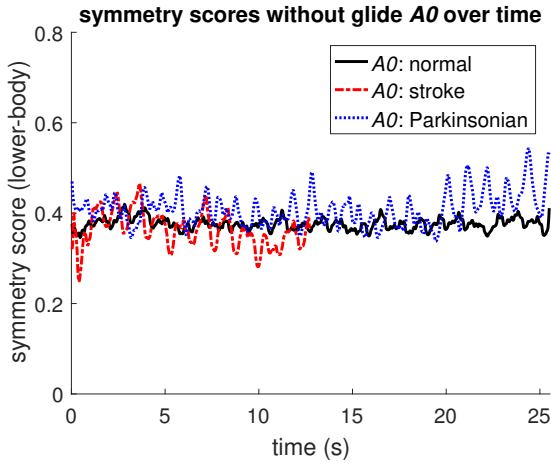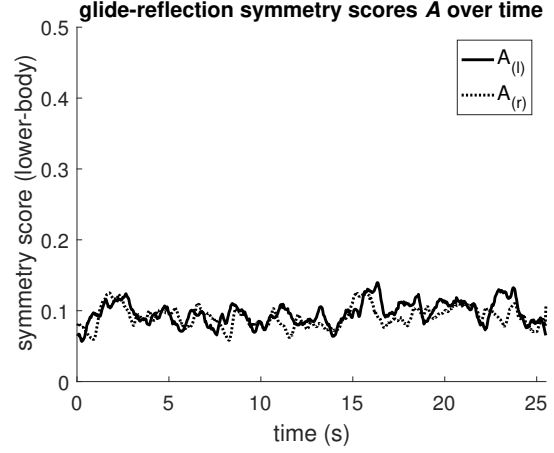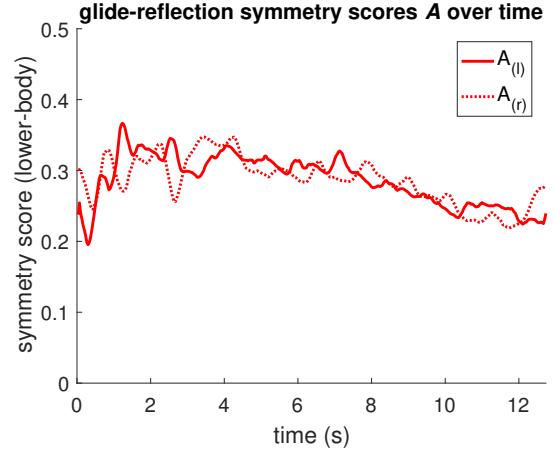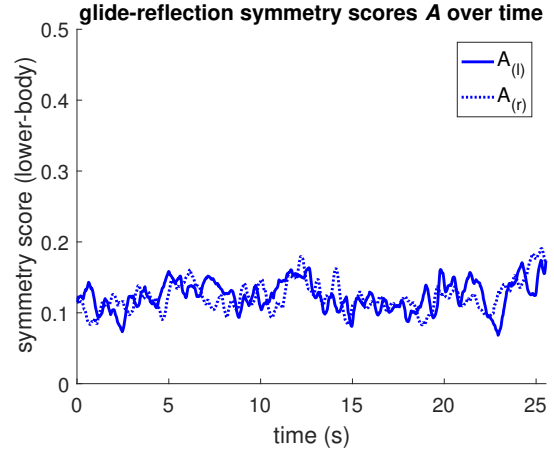

Figure 4: Lower-body symmetry scores without glide $A0_{(l)}$ over one session for each gait type.
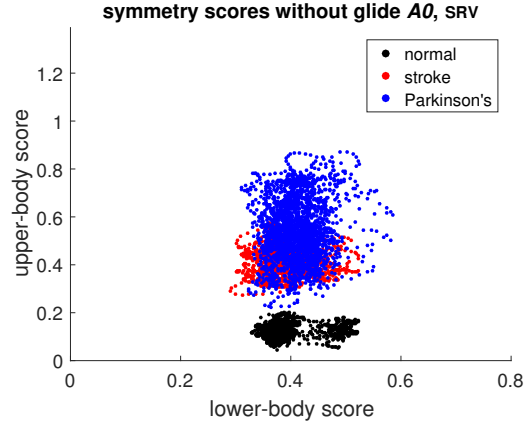

(a) Scores for normal gait
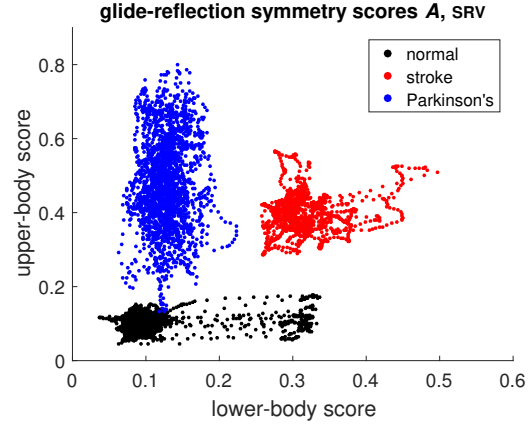

(b) Scores for stroke (hemiplegic) gait
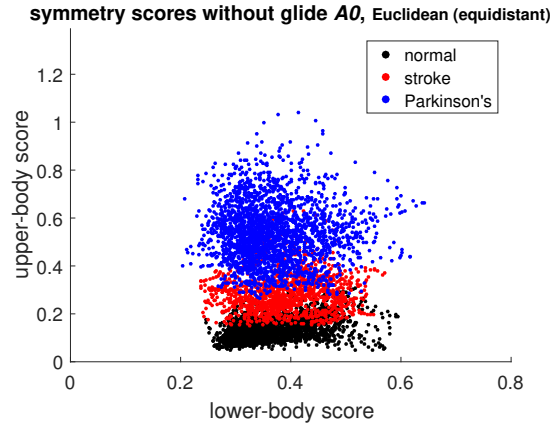

(c) Scores for Parkinsonian gait

Figure 5: Lower-body symmetry scores $A_{(l)}$ and $A_{(r)}$ over one session. Higher scores correspond to less amount of glide-reflection symmetry.
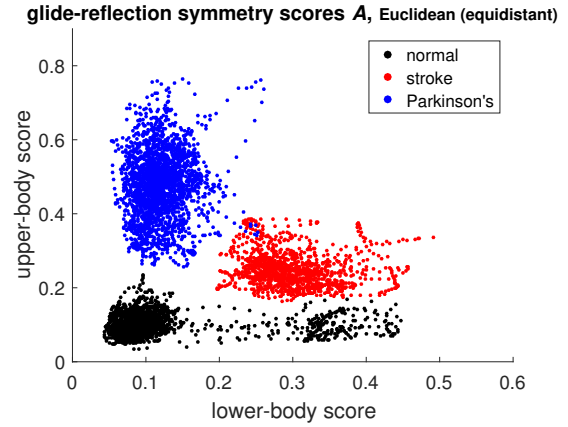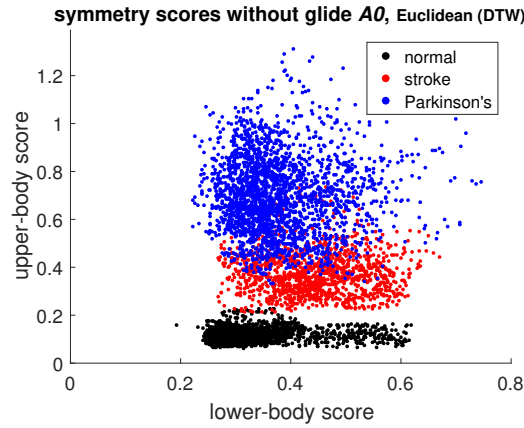
symmetry scores without glide _A0_, SRV

(a) Scores from SRV functions

symmetry scores without glide _A0_, Euclidean (equidistant)

(b) Scores from trajectories in Euclidean space and equidistant resampling

symmetry scores without glide _A0_, Euclidean (DTW)

(c) Scores from trajectories in Euclidean space and DTW

Figure 6: Symmetry scores without glide $A0_{(l)}$ in walking. Each dot is the score at one frame. Higher scores correspond to less amount of glide-reflection symmetry.

glide-reflection symmetry scores _A_, SRV

(a) Scores from SRV functions

glide-reflection symmetry scores _A_, Euclidean (equidistant)

(b) Scores from trajectories in Euclidean space and equidistant resampling

glide-reflection symmetry scores _A_, Euclidean (DTW)

(c) Scores from trajectories in Euclidean space and DTW

Figure 7: Symmetry scores $A_{(l)}$ in walking. Each dot is the score at one frame. Higher scores correspond to less amount of glide-reflection symmetry.

and knees, these additional weights were not used, and $A_{ub} = A_{elbow} + A_{hand}$, and $A_{lb} = A_{knee} + A_{foot}$. For easier comparison, the Euclidean symmetry scores were multiplied by a constant for each approach, such that the average upper-body and lower-body scores for normal gait are the same for all three methods.

The results are shown in Figures 4–7. For clarity, only $A_{(l)}$ or lower-body scores were illustrated. In Figure 4, adding temporal history in spatial symmetry calculation did help "stabilize" the scores, which did not oscillate as much as those in Figure 2. However, without including temporal glide, the lower-body scores for normal and pathological gaits appeared at the same level. Although different movements do not necessarily have to exhibit different degrees of symmetry, from human observation it was obvious that at least the stroke gait was much more asymmetric than the normal gait, both in upper and lower bodies, and the $A0$ scores were not consistent with this observation. By comparison, the glide-reflection symmetry scores in Figure 5 were both stable and more discriminative in a way that was consistent with human perception. It can also be seen that the scores calculated from the left and right sides were closely correlated, as expected.

To compare the scores of different gaits, both upper- and lower-body scores from all 3 sessions were plotted together in Figures 6–7. Each subfigure shows the result from a different method. Once again, the $A0$ scores without glide in Figure 6 did not separate different gait types well. We applied a linear support vector machine (SVM) classifier using leave-one-out cross-validation to predict gait type with just the two composite scores, and the average accuracies were only 85.7%, 88.0%, and 95.2%, respectively.

The glide-reflection symmetry scores we proposed performed much better. It can be seen in Figure 7 that with either our proposed method or the Euclidean approaches, the three different types of gaits were separated quite well just by the two composite scores. The same SVM classifier gave average accuracies of 99.7%, 99.5%, and 100%, respectively. However, it should be emphasized that the symmetry scores are not designed for classification tasks. The main purpose is that a lower score should be obtained when a movement is more symmetric, and the scores should be stable to facilitate smooth feedback. From the results shown in Figure 7, our proposed method provided scores that were more consistent with human perceptions (*e.g.* normal gait has the highest degrees of symmetry in both upper and lower bodies), and exhibited less variance (see Table 1) so that they could generate smoother feedback. This suggested that our proposed method could potentially provide better symmetry scores for the intended applications than Euclidean approaches.

Gait type		Normal	Stroke	Parkinsonian
A_{ub}	Proposed	0.10 ± 0.02	0.40 ± 0.05	0.48 ± 0.12
	Equidistant	0.10 ± 0.03	0.25 ± 0.04	0.48 ± 0.09
	DTW	0.10 ± 0.02	0.35 ± 0.06	0.63 ± 0.12
A_{lb}	Proposed	0.12 ± 0.06	0.32 ± 0.04	0.13 ± 0.02
	Equidistant	0.12 ± 0.08	0.30 ± 0.05	0.12 ± 0.03
	DTW	0.12 ± 0.10	0.35 ± 0.06	0.12 ± 0.03

Table 1: Comparison of glide-reflection symmetry scores $A_{(l)}$ (mean ± standard deviation) from three different metrics.

5. Summary

In this paper we proposed a method to continuously measure the degree of glide-reflection symmetry in human movements, using differential geometric tools from elastic shape analysis. Our preliminary experiment showed that our proposed method worked well to distinguish between normal gait and simulated pathological gaits, and could generate stable outputs to drive feedback systems. However, the current implementation of the method was online but not real-time. Our future work will be focused on applying fast approximate methods to increase the speed of the method and aim for building real-time systems with it.

References

[1] P.-T. Cheng, S.-H. Wu, M.-Y. Liaw, A. M. Wong, and F.-T. Tang. Symmetrical body-weight distribution training in stroke patients and its effect on fall prevention. *Archives of Physical Medicine and Rehabilitation*, 82(12):1650–1654, 2001. 2

[2] M. Eslitzbichler. Modelling character motions on infinite-dimensional manifolds. *The Visual Computer*, 31(9):1179–1190, 2015. 2

[3] M. Field and M. Golubitsky. *Symmetry in chaos: a search for pattern in mathematics, art, and nature*. SIAM, 2009. 2

[4] L. Gorelick, M. Blank, E. Shechtman, M. Irani, and R. Basri. Actions as space-time shapes. *Transactions on Pattern Analysis and Machine Intelligence*, 29(12):2247–2253, December 2007. 1

[5] A. S. Householder. Unitary triangularization of a nonsymmetric matrix. *Journal of the ACM (JACM)*, 5(4):339–342, 1958. 3, 4

[6] S. Joshi, A. Srivastava, E. Klassen, and I. Jermyn. A novel representation for computing geodesics between n-dimensional elastic curves. In *IEEE Conference on Computer Vision and Pattern Recognition (CVPR) June*, 2007. 4

[7] D. G. Kendall. Shape manifolds, procrustean metrics, and complex projective spaces. *Bulletin of the London Mathematical Society*, 16(2):81–121, 1984. 3

[8] S. Lee and Y. Liu. Curved glide-reflection symmetry detection. *IEEE Transactions on Pattern Analysis and Machine Intelligence*, 34(2):266–278, 2012. 2

[9] Y. Liu, R. Collins, and Y. Tsin. Gait sequence analysis using frieze patterns. In *European Conference on Computer Vision*, pages 657–671. Springer, 2002. 2

[10] C. Samir, A. Srivastava, M. Daoudi, and S. Kurtek. On analyzing symmetry of objects using elastic deformations. In *International Conference on Computer Vision Theory and Applications*, pages 194–200, 2009. 2

[11] D. Schattschneider. The plane symmetry groups: their recognition and notation. *The American Mathematical Monthly*, 85(6):439–450, 1978. 2

[12] A. Srivastava, E. Klassen, S. H. Joshi, and I. H. Jermyn. Shape analysis of elastic curves in Euclidean spaces. *IEEE Transactions on Pattern Analysis and Machine Intelligence*, 33(7):1415–1428, 2011. 2, 3

[13] Stanford University School of Medicine. Gait abnormalities. `https://stanfordmedicine25.stanford.edu/the25/gait.html`, 2017. 4

[14] Q. Wang, R. Anirudh, and P. Turaga. Temporal reflection symmetry of human actions: A Riemannian analysis. In *Proceedings of the 1st International Workshop on DIFFerential Geometry in Computer Vision for Analysis of Shapes, Images and Trajectories (DIFF-CV 2015)*, pages 10.1–10.8. BMVA Press, September 2015. 2

[15] H. Zabrodsky, S. Peleg, and D. Avnir. Symmetry as a continuous feature. *IEEE Transactions on Pattern Analysis and Machine Intelligence*, 17(12):1154–1166, 1995. 2

[16] H. Zhou, Q. Wang, T. Ingalls, G. Coleman, and P. Turaga. A home-based system for postural symmetry assessment and training. In *2016 IEEE 38th Annual International Conference of the Engineering in Medicine and Biology Society (EMBC)*. IEEE, 2016. 2

[17] W. Zijlstra. Assessment of spatio-temporal parameters during unconstrained walking. *European Journal of Applied Physiology*, 92(1-2):39–44, 2004. 2